Anti-leukemic activity of microRNA-26a in a chronic lymphocytic leukemia mouse model

Lucilla D'Abundo [1**], Elisa Callegari [1**], Antonella Bresin [1,2], Antonella Chillemi [3,4], Bahaeldin K. Elamin [5,6], Paola Guerriero [1], Xiaomeng Huang [7,8,9], Elena Saccenti [10], Enaam M.A.A. Hussein [1,11], Fabio Casciano [12], Paola Secchiero [12], Giorgio Zauli [12], George A. Calin [13], Giandomenico Russo [2], Ly James Lee [7,8], Carlo Maria Croce [9], Guido Marcucci [14], Silvia Sabbioni [15], Fabio Malavasi [3,4], Massimo Negrini [1*]

1 Department of Morphology, Surgery and Experimental Medicine, University of Ferrara, Ferrara, Italy
2 Laboratorio di Oncologia Molecolare, Istituto Dermopatico dell'Immacolata, IDI-IRCCS, Rome, Italy
3 Laboratory of Immunogenetics, Department of Medical Sciences, University of Torino, Torino 10126, Italy
4 Laboratorio di Immunologia dei Trapianti, Città della Salute e della Scienza, Torino 10126, Italy
5 Microbiology Department, Faculty of Medical laboratory Sciences, University of Khartoum, Sudan
6 Microbiology Department, College of Medicine, University of Bisha, Saudi Arabia
7 Nanoscale Science and Engineering Center for Affordable Nanoengineering of Polymeric Biomedical Devices, The Ohio State University, Columbus, Ohio, USA
8 Department of Chemical and Biomolecular Engineering, The Ohio State University, Columbus, Ohio, USA
9 Comprehensive Cancer Center, The Ohio State University, Columbus, Ohio, USA
10 Hematology Section, Department of Medical Sciences, University of Ferrara, University Hospital Arcispedale S. Anna, Ferrara, Italy
11 Hematology and Immunohematolgy Department, Faculty of Medical laboratory Sciences, University of Khartoum, Sudan
12 Department of Morphology, Surgery, Experimental Medicine and LTTA Centre, University of Ferrara, Ferrara, Italy
13 Department of Experimental Therapeutics, Division of Cancer Medicine, The University of Texas MD Anderson Cancer Center, Houston, TX
14 Gehr Family Center For Leukemia Research Hematologic Malignancies Institute City of Hope, Duarte, CA, 90010, USA
15 Department of Life Sciences and Biotechnology, University of Ferrara, Ferrara, Italy

** LD'A and EC contributed equally to this work

***Corresponding Authors**
Massimo Negrini, PhD
University of Ferrara
Dept of Surgery, Morphology and Experimental Medicine
Via Luigi Borsari, 46
44121 Ferrara, Italy
Phone: +39 0532 455 399
Email: ngm@unife.it

Lucilla D'Abundo, PhD
University of Ferrara
Dept of Surgery, Morphology and Experimental Medicine
Via Luigi Borsari, 46
44121 Ferrara, Italy
Phone: +39 0532 455 871
Email: dbnlll@unife.it

Running Title: Anti-leukemic activity of microRNA-26a in CLL

Abstract

Dysregulation of microRNAs (miRNAs) plays an important role in the pathogenesis of chronic lymphocytic leukemia (CLL). The Eμ-*TCL1* transgenic mouse develops a form of leukemia that is similar to the aggressive type of human B-CLL, and this valuable model has been widely used for testing novel therapeutic approaches. Here, we adopted this model to investigate the potential effects of miR-26a, miR-130an and antimiR-155 in CLL therapy.

Improved delivery of miRNA molecules into CLL cells was obtained by developing a novel system based on lipid nanoparticles conjugated with an anti-CD38 monoclonal antibody. This methodology has proven to be highly effective in delivering miRNA molecules into leukemic cells.

Short and long-term experiments showed that miR-26a, miR-130a and anti-miR-155 increased apoptosis after *in vitro* and *in vivo* treatment. Of this miRNA panel, *miR-26a* was the most effective in reducing leukemic cell expansion. Following long-term treatment, apoptosis was readily detectable by analyzing cleavage of PARP and caspase-7. These effects could be directly attributed to miR-26a, as confirmed by significant downregulation of its proven targets, namely cyclin-dependent kinase 6 and Mcl1.

The results of this study are relevant to two distinct areas. The first is related to the design of a technical strategy and to the selection of CD38 as a molecular target on CLL cells, both consenting efficient and specific intracellular transfer of miRNA. The original scientific finding inferred from the above approach is that miR-26a can elicit *in vivo* anti-leukemic activities mediated by increased apoptosis.

Keywords: miRNA, CLL, Nanoparticles, CD38, miRNA delivery.

Introduction

Chronic lymphocytic leukemia (CLL) is the most common B-cell malignancy in Western countries. CLL lymphocytes resemble memory B cells with a mature phenotype (1). This leukemia is characterized by the accumulation of CD5+ B lymphocytes in the blood, spleen, liver, lymph nodes, and bone marrow. Despite its morphological homogeneity, CLL is a clinically heterogeneous disease (2-4) with a number of adverse factors that affect the clinical course, including stage(5); CD38 positivity; unmutated variable region of the immunoglobulin heavy chain gene (*IGHV*) (6); ZAP70 positivity (7); karyotype aberrations (8); and TP53, NOTCH1, SF3B1, and other gene mutations (9, 10). Despite the progress in chemoimmunotherapy, CLL remains an incurable disease (11).

To help decipher the pathogenic mechanisms of disease and evaluate the efficacy and mechanisms of action of novel therapies, researchers have developed mouse models that resemble human CLL (12, 13). The Eμ-*TCL1* transgenic (*TCL1*-tg) mouse develops a leukemia that is highly similar to the aggressive form of human CLL (14-16). An important feature of *TCL1* overexpression is that it exhibits 100% disease penetrance. At the age of 16–20 months, these mice show a B-CLL-like disease characterized by spleno- and hepatomegaly associated with high counts of white blood cells. Leukemias are characterized by clonal expansion of B cells with a B220+/IgM+/CD5+ immunophenotype, unmutated *IGHV*, increased proliferation, and enhanced AKT phosphorylation. Tumor cells in *TCL1*-tg mice have wild-type (WT) p53 and initially respond to fludarabine treatment (17). Notably, leukemic cells from a *TCL1*-tg donor can be transplanted by intraperitoneal (IP) or intravenous injection into syngeneic WT or immunodeficient mice (e.g., SCID) to accelerate the disease course and generate genetically homogeneous populations of leukemic cells, which better allows for systematic comparison of novel therapies.

MicroRNAs (miRNAs) play a central role in the pathogenesis of CLL. They regulate gene expression at the post-transcriptional level by targeting messenger RNA for degradation or translational inhibition and thus can modulate several biological processes. As a consequence of their deregulation, miRNAs may act as oncogenes or tumor suppressors (18). The discovery of the involvement of miRNAs in human cancer originated from studies of CLL (19). miR-15a and miR-16-1 were found within the minimal region of deletion at chromosome 13q, the most frequent genetic alteration found in human CLL. Deletion of miR-15a/miR-16-1 in a knockout mouse model was shown to confer predisposition to the development of an indolent form of leukemia similar to human CLL (20). BCL2 was a target of these miRNAs; thus, their loss eliminated control over BCL2 expression (21). It is notable that venetoclax, a highly active and recently approved drug against CLL, was designed to inhibit BCL2 activity (22). A prognostic signature consisting of a panel of aberrantly expressed miRNAs has been identified in CLL (23). Other important miRNAs in human CLL include miR-34a, which, being an effector of the p53 protein, is strongly downregulated in 17p-CLL cases, or miR-181b, which is downregulated during disease progression (24-26). In a more recent comprehensive study, we found that a number of miRNAs are deregulated in CLL (27). miRNAs were differentially expressed between CLL cells and mature antigen-experienced B cells, or correlated to specific pathological features (*IGHV* somatic mutations or specific cytogenetic aberrations) or clinical parameters, such as time to first treatment (27). These studies established the groundwork from which miRNA-based therapies, either by restoring or repressing miRNA activity, could be designed and tested. We have already investigated miR-181b as a potential therapeutic molecule against leukemias of the *TCL1*-tg mouse model (28). The study proved that this miRNA induced a measurable anti-leukemic effect. However, an improvement in delivery methods was suggested.

Here, we used the Eμ-*TCL1*FL mouse model (15) to test the anti-leukemic activity of various miRNA mimics or anti-miRNA oligonucleotides (AMOs). To increase *in vivo* delivery, we developed a lipopolyplex formulation that included anti-CD38 conjugated lipid nanoparticles (CD38-NPs), which considerably increased the specificity for hCD38+ leukemic cells of this mouse model. The choice of CD38 as a molecule to target CLL cells was guided by its known importance in CLL (29), as well as its structural characteristics (30) and the evidence of its antibody-mediated internalization (31).

Results

Leukemic cells of the Eμ-*TCL1*FL transgenic mouse are CD38+. Leukemic cells of the Eμ-*TCL1*FL transgenic mouse or transplanted into syngeneic FVB mice are characterized by B220+/CD5dim surface markers (28). Here, we evaluated the expression of CD38. To this end, the splenic lymphocyte population from transgenic or transplanted FVB mice with a high level of disease was first sorted on the basis of physical parameters, and the B220+/CD5dim leukemic population was identified; finally, the lymphocytes within the B220+/CD5dim gate were analyzed for CD38 expression, showing that more than 98% of the cells were positive (**Figure 1**). This analysis not only confirmed that the *TCL1*-tg model exhibits an immunophenotype typical of an aggressive form of B-CLL characterized by high expression of CD38, but it also provided a way to specifically target leukemic cells.

Lipid nanoparticles conjugated with anti-CD38 antibodies can efficiently deliver miRNAs into CLL cells. On the basis of this evidence, we developed lipid nanoparticles conjugated with anti-CD38 antibodies (CD38-NPs) to improve the efficiency of *in vivo* miRNA delivery into leukemic cells. The lipid NP-miRNAs were synthesized as described (32).

We investigated the efficiency of CD38-NPs both *in vitro* and *in vivo*. *In vitro*, we tested whether CD38-NPs could deliver mature miRNAs into murine *TCL1*-tg leukemic cells. We transfected cells with miR-181b mimics, miRNA that we had previously investigated (28). Twenty-four hours after transfection, cells were collected for RNA extraction and the levels of miR-181b measured (**Supplementary Figure 1**). These *in vitro* results indicated that CD38-NPs could efficiently deliver small RNA into leukemic cells and were approximately 2-fold more efficient than unconjugated NPs.

The *TCL1*-tg mouse represented an excellent model for testing *in vivo* delivery efficiency. We quantitatively investigated the delivery of 100 μg of miR-181b in different organs of FVB-*TCL1* transplanted mice. Mice were treated when they exhibited a lymphocyte disease burden of 30-50% as the percentage of leukemic cells in peripheral blood. We tested CD38-NPs, non-conjugated NPs, or Jet-PEI, a formulation used in our previous study (28), in 4 mice for each condition. The nanoparticles were administered by IP injection. After 24 hours, mice were sacrificed and organs collected. Total RNA was isolated from liver, splenocytes, heart, kidneys, thyroid, lungs, muscle, stomach, intestine, brain, and bladder and the expression levels of miR-181b were quantified by digital PCR (**Figure 2A**). Spleen was the most efficiently targeted organ by CD38-NPs, followed by liver. Compared with the physiological levels in these organs, the amount of miR-181b increased more than 300-fold following CD38-NP-mediated delivery. In splenocytes, CD38-NPs induced an 18-fold increase compared with Jet-PEI and a 3-fold increase compared with non-conjugated NPs (**Figure 2B**). All other organs exhibited increased expression levels of miR-181b, generally at lower levels and independent to the type of NP.

The greater delivery mediated by CD38-NPs in spleen and liver of diseased animals was likely attributable to the presence of a high number of CD38+ cells. This conclusion was supported by

the finding that no significant difference of miR-181b in spleen and liver was observed between CD38-NPs and non-conjugated NPs delivery efficacy when experiment was performed in FVB WT mice (**Supplementary Figure 2**). These findings indicated that CD38-NPs were capable of improving efficiency of delivery and specificity of targeting for CD38+ CLL cells.

miR-26a, miR-130a, and anti-miR-155 are selected as potential anti-leukemic molecules. After the delivery efficacy of CD38-NPs was verified *in vivo* and *in vitro*, we tested the potential anti-leukemic effects of a group of selected miRNAs/anti-miRNAs.

From the results of our previous microRNAome study in human CLL (27), we selected a group of miRNAs that were deregulated in human CLL. Herein, we tested miRNA mimics miR-15, miR-16, miR-26a, miR-125a, miR-130a, and miR-34a or AMOs of miR-21, miR-155, and miR-130a. A scrambled RNA oligo was used as a negative control.

First, we investigated the *in vitro* biological activity on leukemic splenocytes isolated from the spleen of Eμ-*TCL1*FL transgenic mice. Leukemic splenocytes were transfected by the use of CD38-NPs and 48 hours after transfection, apoptotic activity was assessed by Annexin V assay **(Figure 3A, supplementary figure 3)**. The highest apoptotic activity was detected in splenocytes treated with miR-26a, miR-125a, anti-miR-155 and miR-130a ($p < 0.05$). The efficiency of transfection of mimics/AMOs was assessed and confirmed in all the samples by analyzing the expression levels of each miRNA (**Figure 3B)**.

Next, for *in vivo* studies, we first evaluated if the CD38-NPs could also mediate a more effective functional outcome than non-conjugated NPs. Given the high pro-apoptotic activity demonstrated *in vitro*, we selected the miR-26a for measuring *in vivo* biological effects. 100 μg of miR-26a mimics was delivered into mice with a high disease burden (30-50% TCL1+ cells in peripheral blood) by using either CD38-NPs or non-conjugated NPs (3 mice in each group). As control, 3 mice with a similar disease burden were treated with a scrambled RNA oligo. After 48 hours from treatment (IP injection), mice were sacrificed and splenocytes isolated to analyze the biological effects. As shown in **Figure 4** , in comparison with non-conjugated NPs, the use of CD38-NPs induced a more effective down-regulation CDK6, a target of miR26a, and a clearer activation of apoptosis, detectable by cleavage of PARP.

Based on these results, we evaluated a number of miRNA mimics/AMOs for their *in vivo* biological activity using CD38-NPs as delivery vehicles. Transplanted mice with a high disease burden (30-50% TCL1+ cells in peripheral blood) were treated with 100 μg of different miRNA mimics or AMOs (at least 3 mice in each group) by using CD38-NPs; as control, 4 mice with a similar disease burden were treated with scrambled miRNA. After 48 hours of a single treatment (IP injection), mice were sacrificed and splenocytes isolated to analyze the effects of miRNAs on apoptosis by the Annexin V assay. As shown in **Figure 5A**, treatment with miR-26a or miR-130a mimics or with anti-miR-155 oligonucleotides induced a significant increase in apoptotic cells compared with control ($p < 0.05$), while several other miRNAs did not exhibit significant differences. Notably, CD38-NP-Empty treated mice exhibited a negligible effect in comparison with control ($p = 0.6$). The efficiency of delivery of mimic/AMOs in splenocytes was confirmed by quantitative PCR in all samples (**Figure 5B**). These results revealed the potential pro-apoptotic activity of miR-26a, miR-130a, and anti-miR-155 against leukemic cells.

miR-26a reduces the expansion of leukemic cells of Eμ-*TCL1* mice. Given the observed pro-apoptotic effects after short-term treatments *in vitro* and *in vivo*, we sought to assess the potential anti-leukemic activity of miR-26a, miR-130a, or anti-miR-155 after 3 weeks of treatment. We performed the experiments by using FVB WT mice transplanted with Eμ-*TCL1*FL leukemic cells

as we have previously described (28). Syngeneic transplantations were performed in 6-week-old mice by IP injection of $5x10^5$ splenocytes, collected from an Eμ-*TCL1*FL transgenic mouse with advanced disease. We monitored the progression of leukemia in transplanted syngeneic mice over time by quantitatively measuring the increase of the human *TCL1* transgene, using a biomarker of transplanted leukemic cells, in DNA isolated from peripheral blood with digital PCR.

Mice were enrolled for treatment at about 8 weeks after transplantation, when leukemic cells reached 15-30% of peripheral blood lymphocytes. At this stage, mice were assigned to 5 groups of treatment with the same schedule of administration (IP injection of 100 μg of miRNA mimics or AMOs 3 times a week for 3 weeks): (1) miR-26a, (2) miR-130a, (3) anti-miR-155, (4) scrambled oligo control, and (5) CD38-NP-Empty nanoparticles. At the beginning of treatment, each group of mice exhibited the same or a very similar arithmetic mean and standard deviation of leukemic burden.

Before starting the treatments and 48 hours after the last treatment, we measured by digital PCR and FACS analysis the percentage of B220+/CD5+ leukemic cells present in the blood. Results of the two assays were in agreement. The differences between percentages of leukemic cells before and after treatment are shown in **Figure 6**. miR-26a treatment was the most effective in reducing the accumulation/expansion of leukemic cells in blood. The other molecules also induced a reduction of the leukemic cell burden in blood, albeit to a significantly less extent (**Figure 6**).

miR-26a promotes apoptosis in CLL cells. Given the significant anti-leukemic effect of miR-26a, we investigated the effect of miR-26a on leukemic splenocytes after 3 weeks of *in vivo* treatment.

The activation of apoptosis was clearly detectable by analysis of poly(ADP-ribose) polymerase (PARP) and caspase-7: the appearance of the 85-kD fragment (cleaved PARP), together with the strong increase in cleavage of caspase-7 were seen only in mice treated with CD38-NP-miR-26a, thus indicating the induction of apoptosis **(Figure 7A)**.

To confirm that the apoptotic effect could be attributable to miR-26a activity, we analyzed the levels of two of its targets, Mcl1 and cyclin-dependent kinase 6 (Cdk6). Treatment with CD38-NP-miR-26a induced their downregulation, thus confirming the molecular activity of the delivered miR-26a **(Figure 7B)**.

Discussion

The aim of this study was to demonstrate that miRNA-based therapies may have a place in the treatment of CLL, a human leukemia that is still incurable despite recent multiple successes. Our approach was based on evidence related to aberrant expressions of miRNA in CLL and on numerous observations (19, 23, 25, 27, 33).

To address the working hypothesis, we adopted the Eμ-*TCL1* mouse model, which develops a leukemia that is highly similar to an aggressive form of human CLL (15, 16). Using this model, we previously reported the anti-leukemic activity of miR-181b mimics (28). Here, we assayed miR-15a, miR-16-1, miR-26a, miR-125a, miR-130a, miR-34a, ant-miR-130a, anti-miR-21, and anti-miR-155. Among these, miR-26a, miR-130a, and anti-miR-155 induced apoptosis in leukemic cells both *in vitro* and *in vivo* in short-term assays. On the basis of these results, we tested the ability of miR-26a, miR-130a, and anti-miR-155 to counteract the *in vivo* accumulation/expansion of leukemic cells of the Eμ-*TCL1* mouse model.

miR-155 is a well-known oncomiR (34-39). In human CLL, a high level of miR-155 was associated with various adverse prognostic factors (27, 40-43). Overexpression of miR-155 in transgenic mice

was shown to induce polyclonal B-cell expansion (34). The use of anti-miR-155 molecules has been reported to significantly decrease *in vivo* tumor growth of BCWM1 cells derived from a patient with Waldenstrom macroglobulinemia (44). The role of miR-130a in tumorigenesis is, on the other hand, controversial. Various reports have indicated either tumor-suppressive (45-51) or oncogenic (52-56) activity, depending on the experimental settings. In human CLL, miR-130a was shown to repress a survival autophagic pathway by targeting ATG2B and DICER1 (57). No animal models are available to examine the physiological or pathological function of miR-130a. Similarly, contrasting results of dysregulated miR-26a have been reported in different tumor types (58-60). For example, it was shown that miR-26a could facilitate glioblastoma formation *in vivo* (58, 61), but it was also shown that low miR-26a expression conferred a shorter overall survival in liver cancer patients (62) and that its delivery through an adeno-associated viral vector could achieve a therapeutic effect on a MYC-induced liver cancer mouse model (59). In human CLL, a tumor suppressive function of miR-26a was supported by evidence that its low expression was associated with a shortened time from diagnosis to first treatment (27), a clinical feature associated with poor prognosis.

Despite the limited evidence linking miR-26a to CLL pathogenesis, this miRNA exhibited the strongest activity against the accumulation/expansion of leukemic cells by enhancing apoptosis. Several studies have previously documented that miR-26a is able to target and down-modulate several protein-coding gene targets, including CDK6, cyclins D2/E2, and Mcl-1, in different tumor cells (59, 63-65). Here, we found that a strong apoptotic effect was detectable in the spleen of treated mice and proof of miR-26a activity was confirmed by the downregulation of two of its known targets, Mcl1 and Cdk6. The concomitant downregulation of the anti-apoptotic Mcl1 and the cell cycle-promoting Cdk6 proteins suggests not only that miR-26a can promote apoptosis, but that it can also inhibit CLL cell proliferation.

A second important result of this study was the development of nanoparticles conjugated with anti-CD38 antibodies that could efficiently deliver miRNA or AMOs into CD38+ cells, which typically characterize the most aggressive forms of CLL (29) and other hematological diseases such as myeloma. In fact, efficient, specific, and safe delivery of miRNA mimics or AMOs is a major challenge in miRNA-based therapeutic applications (66, 67).

Currently, methods for miRNA systemic delivery are mainly designed to target the liver (68, 69) and they may use either viral (59, 70, 71) or non-viral systems (72-76). Significant therapeutic effects in murine liver cancer models have been described (59, 70, 77). More difficult, however, is the systemic delivery of miRNA mimics to other organs or tissues. Regarding hematopoietic cells, *in vivo* delivery of antagomiR-126 was achieved in acute myeloid leukemia subpopulations by using lipopolyplex nanoparticles conjugated with transferrin or antibody (anti-CD45.2) (72). The chemical and physical characteristics of this formulation were shown to bypass hepatic uptake and ultimately achieve better delivery to hematopoietic organs (32). An analogous system based on stable nucleic acid lipid vesicles conjugated with transferrin was developed to target multiple myeloma cells expressing transferrin receptors (78, 79).

To develop a method for *in vivo* delivery to CLL cells, here we produced lipid nanoparticles, based on the formulation by Huang *et al* (32), conjugated with an anti-CD38 antibody, whose antigen is present on the surface of leukemic cells of Eμ-*TCL1* mouse model. Delivery to leukemic cells was superior to that of either non-conjugated nanoparticles or JetPEI, the nanosystem that we used in our previous report (28). The presence of the anti-CD38 antibody conferred specificity of action and also led to internalization of the nanoparticle complex in targeted leukemic spleen cells. The internalization was previously shown by using a panel of rat and mouse-anti CD38 mAbs (31). The

results indicated that the adopted methodology is efficient in transferring a cargo of different miRNAs to leukemic cells. This competence was maintained *in vivo*. Spleen and liver were the most efficiently targeted organs by CD38-NPs. A small increase of miR-181b was also detectable in other organs, especially when non-conjugated nanoparticles were used. Since diseased mice are characterized by spleno- and hepatomegaly, these results strongly suggested that the CD38-NPs could increase delivery efficiency to these organs because they accumulate CD38+ CLL cells. The characteristics of CD38 targeting in terms of safety were recently confirmed *in vivo* in mAb-mediated therapy of human myeloma (80).

The main result of this study is that miR-26 exhibits a clear apoptotic effect on leukemic cells and a significant reduction in leukemic cell expansion, suggesting its consideration for future CLL therapy, possibly in combination with presently used therapeutic approaches. Moreover, we provide a novel delivery method, which improves the efficiency and specificity of miRNA delivery into CD38+ CLL cells. In humans, this approach could help target not only CLL cells in lymphatic organs, but also other CD38+ B-cell malignancies, including various types of lymphoma, plasma cell-derived neoplasms, and acute myeloid leukemia of the t(6;9) subtype (81-86).

Materials and Methods

Cell cultures and transfections. Mouse splenocytes were freshly isolated from diseased mice by using the procedure described by Bresin et al.(28). Transient transfections were performed with 100 nM pre-miR (Ambion) or single-stranded anti-miRNA (IDT) or scrambled negative controls complexed with lipidic nanoparticles (NPs or CD38-NPs). Cells were harvested 48 hours after transfection to evaluate apoptosis and miR expression.

Mice and syngeneic transplantation. The *TCL1*-tg mouse model used for these experiments has been previously described (15). Breeding pairs were provided to our group as a generous gift from C. M. Croce (Ohio State University). FVB WT mice were obtained from Charles River Laboratories. Mice had ad libitum access to water and a pellet diet. The animal room was maintained at 23°C on a 12-h light/12-h dark cycle. At the age of 6 weeks, the WT FVB female mice were transplanted by IP injection of $5x10^5$ lymphocytes isolated from the spleen of an adult *TCL1*-tg mouse with established leukemia. The engraftment of leukemic cells and the progression of disease were monitored over time by the expression of B220/CD5 using flow cytometry analysis (FACS) or absolute quantification of the human *TCL1* transgene by digital PCR of peripheral blood DNA. In order to comply with the 2010/63/EU directive of the European Parliament and Council, enforced by the Italian law, which requires that the number of experimental animals be minimized, for long term experiments, G*Power (http://www.gpower.hhu.de/) was used to define sample size. For short term experiments, the smallest number of mice sufficient to perform statistical analyses was used. All animals were randomly assigned to different treatment groups at the start of the studies. The protocol for animal experimentation was approved by the Italian Ministry of Health (approval n. 40-2014 PR released on November 6, 2014).

Anti-CD38 monoclonal antibody. The anti-CD38 antibody is a rat monoclonal antibody (mAb) specific for mouse CD38 antigen. It was produced in the laboratory of one of the authors (FM, University of Turin). The NIMR-5 clone was expanded *in vitro* in Iscove's Modified Dulbecco's Medium and purified by high pressure liquid chromatography. The purified IgG was then sterilized by 0.22-µm filtration (Millipore Polyethersulfone Millex-GP Syringe Filter Unit, radiosterilized) and detoxified by Detoxi-Gel Endotoxin Removing Gel (Thermo Scientific) (87). Specificity was

confirmed by reacting the purified mAb with the murine X63.Ag8 myeloma cell line and analyzing binding by indirect immunofluorescence (87).

Preparation of nanoparticles. The lipid components of the nanoparticles were 1,2-dioleoyl-sn-glycero-3-phosphoethanolamine (DOPE), 1,2-dimyristoyl-sn-glycerol, methoxypolyethylene glycol (MW ~2000; DMG-PEG; Avanti Polar Lipids, Alabaster, AL), and linoleic acid (Sigma-Aldrich, St. Louis, MO). The molar ratio of DOPE:linoleic acid:DMG-PEG was 50:48:2. The preparation of empty nanoparticles was performed as previously described (32). The anti-CD38 antibody was conjugated with 1,2-distearoyl-sn-glycero-3-phosphoethanolamine-N-[maleimide (polyethylene glycol)-2000] (DSPE-PEG2000 maleimide) according to the method described in a previous study (72) and was then post-inserted into the surface of lipopolyplex nanoparticles to form the CD38-NP-miRs.

***In vivo* treatment with mimics or AMOs.** The synthetic mimics and anti-miRNAs for *in vivo* delivery were purchased from Axolab (Germany). For short-term experiments, the FVB mice (at least 3 mice in each group) were randomly enrolled for treatment when the disease reached 30-50% of *TCL1*-positive cells in peripheral blood, and they were treated once with 100 μg of specific single-strand mimics/anti-miRNA and sacrificed after 48 hours. For long-term experiments, the mice (at least 6 mice in each group) were randomly enrolled for treatment when the disease reached 15-30% of *TCL1*-positive cells in peripheral blood, and they were treated with 100 μg of the specified molecules 3 times a week for 3 weeks. For long-term treatments, the levels of disease were measured by FACS and droplet digital PCR (ddPCR) analysis the day before the start of treatment and 48 hours after it ended.

Flow cytometry. Blood samples (20 μL) were placed in a tube containing 0.5 M EDTA as an anticoagulant. Erythrocytes were lysed by treatment with ammonium chloride (0.8%) and EDTA (0.1 mM) (Sigma). Cells were incubated with specific antibodies for 10 min in ice, washed, and analyzed by flow cytometry in a FACSCalibur flow cytometer (Becton Dickinson, San Jose, California, USA) by using FlowJo software (TreeStar, Ashland, OR). Data for $5x10^4$ cells within the lymphocyte light-scatter gate were collected. In these assays, color compensation was performed before cell acquisition by using the MACS Comp Bead Kit, anti-rat Igκ (Miltenyi Biotec, Gladbach, Germany). During analysis, gates were set by using a Fluorescence Minus One control strategy. Leukemic cells were identified as B220+/CD5dim cells, normal B lymphocytes as B220+/CD5- cells, and T lymphocytes as B220-/CD5+ cells. The following antibodies were used: FITC rat anti-mouse CD5 (Cat. 553020, BD Pharmingen) and PeCy5 rat anti-mouse CD45R/B220 (Cat. 553091, BD Pharmingen). CD38 expression on the surface of leukemic splenocytes was detected by triple staining using a PE rat anti-mouse CD38 antibody (Cat. 130-103-008, Miltenyi Biotec) together with the FITC rat anti-mouse CD5 and the PeCy5 rat anti-mouse CD45R/B220 antibody indicated above.

Analysis of apoptosis. The apoptotic effect of mimic or anti-miR molecules on murine splenocytes treated *in vitro* or *in vivo* was assessed by the Muse™ Annexin V and Dead Cell Assay kit (Cat. MCH100105, Merck) according to manufacturer's protocol. To count viable cells, we used the Muse Count & Viability Assay kit (Cat. MHC100102, Merck).

RNA and DNA extraction. Total RNA and DNA were isolated from cells or tissues by using the Maxwell Rapid Sample Concentrator (RSC) Instrument (Promega) with the Maxwell RSC miRNA Tissue Kit and the Maxwell RSC Blood DNA Kit.

Reverse transcription and ddPCR. The ddPCR method was used to measure the expression level of miRNAs. The reverse transcription reaction was performed on 5 ng of total RNA by using the TaqMan miRNA Reverse Transcription assay. After appropriate dilution, 1 μL of the cDNA was used

for amplification in a 20-µL reaction volume containing ddPCR Supermix for Probes (Bio-Rad) and the TaqMan miRNA PCR probe set. Droplets generation, cycling conditions for TaqMan assays and the counting of positive droplets were performed according to procedures described by Miotto et al. (88). To normalize the relative abundance of miRNAs, we used the Taqman Assays for RNAs U6 or SNO412 (Applied Biosystems).

Monitoring leukemic cells by ddPCR. A ddPCR approach was used to measure the human *TCL1* transgene in DNA extracted from peripheral blood cells of FVB transplanted mice. We used primers/probes specific for the human *TCL1* transgene (forward 5'-CTCTGGCTCTTGCTTCTTAG-3'; reverse 5'-CACCCGTAACTGTAACCTATC-3'; probe--/56-FAM/TCGTGTATT/Zen/TGGACGAGAAGCA GCA/3IABkFQ/) and primers/probes specific for the mouse *Gapdh* gene as an endogenous reference (forward 5'-GGTGTGAACCACGAGAAATA-3'; reverse 5'-CTCATGGCAGGGTAAGATAAG-3'; probe--/5HEX/ACAAC TTTG/Zen/GCATTGTGGAAGGGC/3IABkFQ/). The probes for human *TCL1* and mouse *Gapdh* were conjugated with FAM and HEX, respectively. The ddPCR assay was performed on 10 ng of genomic DNA, using the same procedures as described above.

Western blot analysis. Splenocytes of treated and control mice were suspended in radioimmunoprecipitation assay (RIPA) buffer (Sigma-Aldrich), supplemented with protease and phosphatase inhibitors (Sigma-Aldrich), according to the manufacturer's protocol. Protein concentrations were measured with the Bradford assay (Bio-Rad). Equal amounts (30 µg) of protein extracts from all samples were applied to SDS-PAGE electrophoresis and then transferred to a PVDF membrane (Bio-Rad). The membrane was incubated with primary antibodies as follows: anti-CDK6 (rabbit, Cat. sc177, Santa Cruz), anti-Mcl-1 (Rabbit, Cat.5453 Cell Signalling) , anti-PARP (rabbit, Cat. 9542, Cell Signalling) , anti-caspase-7 (rabbit, Cat. 9492, Cell Signaling) 1:1000. β-Tubulin H235 (rabbit, Cat. sc9104, Santa Cruz), , was used as a normalized control. The membrane was incubated with anti-rabbit IgG, HRP-linked antibody (Cat. 7074, Cell Signaling). For signal detection, Clarity™ Western ECL Substrate (Cat. 170-5060, Bio-Rad) was used according to the manufacturer's instructions. Digital images were acquired with Chemidoc (BioRad). Signals were quantified by ImageJ software and protein expression levels normalized according to β-tubulin expression.

Statistical analyses. Reported data are expressed as mean ± SD; the calculated t-test or t-test with Welch's correction when required were considered statistically significant at p-value < 0.05. Variances between groups were evaluated by the F-test. Graphpad Prism 6.0 software was used for data analysis. No samples or animals were excluded from the analyses. None of the investigators were blinded to group allocations.

Conflict of Interest: The authors declare no competing financial interests.

Acknowledgements

This work was supported by funds from the Italian Association for Cancer Research (AIRC Special program 5xmille n.9980) and the University of Ferrara to MN, from the US National Cancer Institute grant CA19-7706 to CMC, from FIRB Programme of the Ministry of University and Research (Rome, Italy), Fondazione Cassa di Risparmio di Torino and Fondazione Ricerca Molinette Torino to FM.

Supplementary Information accompanies the paper on the *Oncogene* website (http://www.nature.com/onc)

Reference

1. Chiorazzi N, Rai KR, Ferrarini M. Chronic lymphocytic leukemia. The New England journal of medicine. 2005;352(8):804-15.
2. Zenz T, Mertens D, Kuppers R, Dohner H, Stilgenbauer S. From pathogenesis to treatment of chronic lymphocytic leukaemia. Nature reviews Cancer. 2010;10(1):37-50.
3. Chiorazzi N, Hatzi K, Albesiano E. B-cell chronic lymphocytic leukemia, a clonal disease of B lymphocytes with receptors that vary in specificity for (auto)antigens. Annals of the New York Academy of Sciences. 2005;1062:1-12.
4. Grever MR, Lucas DM, Dewald GW, Neuberg DS, Reed JC, Kitada S, et al. Comprehensive assessment of genetic and molecular features predicting outcome in patients with chronic lymphocytic leukemia: results from the US Intergroup Phase III Trial E2997. Journal of clinical oncology : official journal of the American Society of Clinical Oncology. 2007;25(7):799-804.
5. Binet JL, Auquier A, Dighiero G, Chastang C, Piguet H, Goasguen J, et al. A new prognostic classification of chronic lymphocytic leukemia derived from a multivariate survival analysis. Cancer. 1981;48(1):198-206.
6. Damle RN, Wasil T, Fais F, Ghiotto F, Valetto A, Allen SL, et al. Ig V gene mutation status and CD38 expression as novel prognostic indicators in chronic lymphocytic leukemia. Blood. 1999;94(6):1840-7.
7. Wiestner A, Rosenwald A, Barry TS, Wright G, Davis RE, Henrickson SE, et al. ZAP-70 expression identifies a chronic lymphocytic leukemia subtype with unmutated immunoglobulin genes, inferior clinical outcome, and distinct gene expression profile. Blood. 2003;101(12):4944-51.
8. Dohner H, Stilgenbauer S, Benner A, Leupolt E, Krober A, Bullinger L, et al. Genomic aberrations and survival in chronic lymphocytic leukemia. The New England journal of medicine. 2000;343(26):1910-6.
9. Landau DA, Tausch E, Taylor-Weiner AN, Stewart C, Reiter JG, Bahlo J, et al. Mutations driving CLL and their evolution in progression and relapse. Nature. 2015;526(7574):525-30.
10. Rossi D, Bruscaggin A, Spina V, Rasi S, Khiabanian H, Messina M, et al. Mutations of the SF3B1 splicing factor in chronic lymphocytic leukemia: association with progression and fludarabine-refractoriness. Blood. 2011;118(26):6904-8.
11. Cuneo A, Cavazzini F, Ciccone M, Daghia G, Sofritti O, Saccenti E, et al. Modern treatment in chronic lymphocytic leukemia: impact on survival and efficacy in high-risk subgroups. Cancer medicine. 2014;3(3):555-64.
12. Simonetti G, Bertilaccio MT, Ghia P, Klein U. Mouse models in the study of chronic lymphocytic leukemia pathogenesis and therapy. Blood. 2014;124(7):1010-9.
13. Bresin A, D'Abundo L, Narducci MG, Fiorenza MT, Croce CM, Negrini M, et al. TCL1 transgenic mouse model as a tool for the study of therapeutic targets and microenvironment in human B-cell chronic lymphocytic leukemia. Cell death & disease. 2016;7:e2071.
14. Bichi R, Shinton SA, Martin ES, Koval A, Calin GA, Cesari R, et al. Human chronic lymphocytic leukemia modeled in mouse by targeted TCL1 expression. Proceedings of the National Academy of Sciences of the United States of America. 2002;99(10):6955-60.
15. Efanov A, Zanesi N, Nazaryan N, Santanam U, Palamarchuk A, Croce CM, et al. CD5+CD23+ leukemic cell populations in TCL1 transgenic mice show significantly increased proliferation and Akt phosphorylation. Leukemia. 2010;24(5):970-5.
16. Yan XJ, Albesiano E, Zanesi N, Yancopoulos S, Sawyer A, Romano E, et al. B cell receptors in TCL1 transgenic mice resemble those of aggressive, treatment-resistant human chronic lymphocytic leukemia. Proceedings of the National Academy of Sciences of the United States of America. 2006;103(31):11713-8.
17. Johnson AJ, Lucas DM, Muthusamy N, Smith LL, Edwards RB, De Lay MD, et al. Characterization of the TCL-1 transgenic mouse as a preclinical drug development tool for human chronic lymphocytic leukemia. Blood. 2006;108(4):1334-8.
18. Negrini M, Ferracin M, Sabbioni S, Croce CM. MicroRNAs in human cancer: from research to therapy. Journal of cell science. 2007;120(Pt 11):1833-40.

19. Calin GA, Dumitru CD, Shimizu M, Bichi R, Zupo S, Noch E, et al. Frequent deletions and down-regulation of micro- RNA genes miR15 and miR16 at 13q14 in chronic lymphocytic leukemia. Proceedings of the National Academy of Sciences of the United States of America. 2002;99(24):15524-9.
20. Klein U, Lia M, Crespo M, Siegel R, Shen Q, Mo T, et al. The DLEU2/miR-15a/16-1 cluster controls B cell proliferation and its deletion leads to chronic lymphocytic leukemia. Cancer cell. 2010;17(1):28-40.
21. Cimmino A, Calin GA, Fabbri M, Iorio MV, Ferracin M, Shimizu M, et al. miR-15 and miR-16 induce apoptosis by targeting BCL2. Proceedings of the National Academy of Sciences of the United States of America. 2005;102(39):13944-9.
22. Roberts AW, Davids MS, Pagel JM, Kahl BS, Puvvada SD, Gerecitano JF, et al. Targeting BCL2 with Venetoclax in Relapsed Chronic Lymphocytic Leukemia. The New England journal of medicine. 2016;374(4):311-22.
23. Calin GA, Ferracin M, Cimmino A, Di Leva G, Shimizu M, Wojcik SE, et al. A MicroRNA signature associated with prognosis and progression in chronic lymphocytic leukemia. The New England journal of medicine. 2005;353(17):1793-801.
24. Fabbri M, Bottoni A, Shimizu M, Spizzo R, Nicoloso MS, Rossi S, et al. Association of a microRNA/TP53 feedback circuitry with pathogenesis and outcome of B-cell chronic lymphocytic leukemia. JAMA : the journal of the American Medical Association. 2011;305(1):59-67.
25. Visone R, Veronese A, Rassenti LZ, Balatti V, Pearl DK, Acunzo M, et al. miR-181b is a biomarker of disease progression in chronic lymphocytic leukemia. Blood. 2011;118(11):3072-9.
26. He L, He X, Lim LP, de Stanchina E, Xuan Z, Liang Y, et al. A microRNA component of the p53 tumour suppressor network. Nature. 2007;447(7148):1130-4.
27. Negrini M, Cutrona G, Bassi C, Fabris S, Zagatti B, Colombo M, et al. microRNAome expression in chronic lymphocytic leukemia: comparison with normal B cell subsets and correlations with prognostic and clinical parameters. Clinical cancer research : an official journal of the American Association for Cancer Research. 2014;20(15):4141-53.
28. Bresin A, Callegari E, D'Abundo L, Cattani C, Bassi C, Zagatti B, et al. miR-181b as a therapeutic agent for chronic lymphocytic leukemia in the Emicro-TCL1 mouse model. Oncotarget. 2015;6(23):19807-18.
29. Malavasi F, Deaglio S, Damle R, Cutrona G, Ferrarini M, Chiorazzi N. CD38 and chronic lymphocytic leukemia: a decade later. Blood. 2011;118(13):3470-8.
30. Malavasi F, Deaglio S, Funaro A, Ferrero E, Horenstein AL, Ortolan E, et al. Evolution and function of the ADP ribosyl cyclase/CD38 gene family in physiology and pathology. Physiological reviews. 2008;88(3):841-86.
31. Chillemi A, Zaccarello G, Quarona V, Ferracin M, Ghimenti C, Massaia M, et al. Anti-CD38 antibody therapy: windows of opportunity yielded by the functional characteristics of the target molecule. Mol Med. 2013;19:99-108.
32. Huang X, Schwind S, Yu B, Santhanam R, Wang H, Hoellerbauer P, et al. Targeted delivery of microRNA-29b by transferrin-conjugated anionic lipopolyplex nanoparticles: a novel therapeutic strategy in acute myeloid leukemia. Clinical cancer research : an official journal of the American Association for Cancer Research. 2013;19(9):2355-67.
33. Calin GA, Pekarsky Y, Croce CM. The role of microRNA and other non-coding RNA in the pathogenesis of chronic lymphocytic leukemia. Best practice & research Clinical haematology. 2007;20(3):425-37.
34. Costinean S, Zanesi N, Pekarsky Y, Tili E, Volinia S, Heerema N, et al. Pre-B cell proliferation and lymphoblastic leukemia/high-grade lymphoma in E(mu)-miR155 transgenic mice. Proceedings of the National Academy of Sciences of the United States of America. 2006;103(18):7024-9.
35. O'Connell RM, Rao DS, Chaudhuri AA, Boldin MP, Taganov KD, Nicoll J, et al. Sustained expression of microRNA-155 in hematopoietic stem cells causes a myeloproliferative disorder. The Journal of experimental medicine. 2008;205(3):585-94.
36. Tagawa H, Ikeda S, Sawada K. Role of microRNA in the pathogenesis of malignant lymphoma. Cancer science. 2013;104(7):801-9.

37. Mattiske S, Suetani RJ, Neilsen PM, Callen DF. The oncogenic role of miR-155 in breast cancer. Cancer epidemiology, biomarkers & prevention : a publication of the American Association for Cancer Research, cosponsored by the American Society of Preventive Oncology. 2012;21(8):1236-43.
38. Zanesi N, Pekarsky Y, Trapasso F, Calin G, Croce CM. MicroRNAs in mouse models of lymphoid malignancies. Journal of nucleic acids investigation. 2010;1(1):36-40.
39. Garzon R, Croce CM. MicroRNAs in normal and malignant hematopoiesis. Current opinion in hematology. 2008;15(4):352-8.
40. Cui B, Chen L, Zhang S, Mraz M, Fecteau JF, Yu J, et al. MicroRNA-155 influences B-cell receptor signaling and associates with aggressive disease in chronic lymphocytic leukemia. Blood. 2014;124(4):546-54.
41. Visone R, Rassenti LZ, Veronese A, Taccioli C, Costinean S, Aguda BD, et al. Karyotype-specific microRNA signature in chronic lymphocytic leukemia. Blood. 2009;114(18):3872-9.
42. Rossi S, Shimizu M, Barbarotto E, Nicoloso MS, Dimitri F, Sampath D, et al. microRNA fingerprinting of CLL patients with chromosome 17p deletion identify a miR-21 score that stratifies early survival. Blood. 2010;116(6):945-52.
43. Vargova K, Curik N, Burda P, Basova P, Kulvait V, Pospisil V, et al. MYB transcriptionally regulates the miR-155 host gene in chronic lymphocytic leukemia. Blood. 2011;117(14):3816-25.
44. Zhang Y, Roccaro AM, Rombaoa C, Flores L, Obad S, Fernandes SM, et al. LNA-mediated anti-miR-155 silencing in low-grade B-cell lymphomas. Blood. 2012;120(8):1678-86.
45. Zhu X, Zhao H, Lin Z, Zhang G. Functional studies of miR-130a on the inhibitory pathways of apoptosis in patients with chronic myeloid leukemia. Cancer gene therapy. 2015;22(12):573-80.
46. Acunzo M, Visone R, Romano G, Veronese A, Lovat F, Palmieri D, et al. miR-130a targets MET and induces TRAIL-sensitivity in NSCLC by downregulating miR-221 and 222. Oncogene. 2012;31(5):634-42.
47. Pan Y, Wang R, Zhang F, Chen Y, Lv Q, Long G, et al. MicroRNA-130a inhibits cell proliferation, invasion and migration in human breast cancer by targeting the RAB5A. International journal of clinical and experimental pathology. 2015;8(1):384-93.
48. Li Y, Challagundla KB, Sun XX, Zhang Q, Dai MS. MicroRNA-130a associates with ribosomal protein L11 to suppress c-Myc expression in response to UV irradiation. Oncotarget. 2015;6(2):1101-14.
49. Fujita Y, Kojima T, Kawakami K, Mizutani K, Kato T, Deguchi T, et al. miR-130a activates apoptotic signaling through activation of caspase-8 in taxane-resistant prostate cancer cells. The Prostate. 2015;75(14):1568-78.
50. Li B, Huang P, Qiu J, Liao Y, Hong J, Yuan Y. MicroRNA-130a is down-regulated in hepatocellular carcinoma and associates with poor prognosis. Med Oncol. 2014;31(10):230.
51. Boll K, Reiche K, Kasack K, Morbt N, Kretzschmar AK, Tomm JM, et al. MiR-130a, miR-203 and miR-205 jointly repress key oncogenic pathways and are downregulated in prostate carcinoma. Oncogene. 2013;32(3):277-85.
52. Shen S, Guo X, Yan H, Lu Y, Ji X, Li L, et al. A miR-130a-YAP positive feedback loop promotes organ size and tumorigenesis. Cell research. 2015;25(9):997-1012.
53. Lee SH, Jung YD, Choi YS, Lee YM. Targeting of RUNX3 by miR-130a and miR-495 cooperatively increases cell proliferation and tumor angiogenesis in gastric cancer cells. Oncotarget. 2015;6(32):33269-78.
54. Chen J, Yan D, Wu W, Zhu J, Ye W, Shu Q. MicroRNA-130a promotes the metastasis and epithelial-mesenchymal transition of osteosarcoma by targeting PTEN. Oncology reports. 2016;35(6):3285-92.
55. Jiang H, Yu WW, Wang LL, Peng Y. miR-130a acts as a potential diagnostic biomarker and promotes gastric cancer migration, invasion and proliferation by targeting RUNX3. Oncology reports. 2015;34(3):1153-61.
56. Liu L, Nie J, Chen L, Dong G, Du X, Wu X, et al. The oncogenic role of microRNA-130a/301a/454 in human colorectal cancer via targeting Smad4 expression. PloS one. 2013;8(2):e55532.
57. Kovaleva V, Mora R, Park YJ, Plass C, Chiramel AI, Bartenschlager R, et al. miRNA-130a targets ATG2B and DICER1 to inhibit autophagy and trigger killing of chronic lymphocytic leukemia cells. Cancer research. 2012;72(7):1763-72.

58. Kim H, Huang W, Jiang X, Pennicooke B, Park PJ, Johnson MD. Integrative genome analysis reveals an oncomir/oncogene cluster regulating glioblastoma survivorship. Proceedings of the National Academy of Sciences of the United States of America. 2010;107(5):2183-8.
59. Kota J, Chivukula RR, O'Donnell KA, Wentzel EA, Montgomery CL, Hwang HW, et al. Therapeutic microRNA delivery suppresses tumorigenesis in a murine liver cancer model. Cell. 2009;137(6):1005-17.
60. Sander S, Bullinger L, Klapproth K, Fiedler K, Kestler HA, Barth TF, et al. MYC stimulates EZH2 expression by repression of its negative regulator miR-26a. Blood. 2008;112(10):4202-12.
61. Huse JT, Brennan C, Hambardzumyan D, Wee B, Pena J, Rouhanifard SH, et al. The PTEN-regulating microRNA miR-26a is amplified in high-grade glioma and facilitates gliomagenesis in vivo. Genes & development. 2009;23(11):1327-37.
62. Ji J, Shi J, Budhu A, Yu Z, Forgues M, Roessler S, et al. MicroRNA expression, survival, and response to interferon in liver cancer. The New England journal of medicine. 2009;361(15):1437-47.
63. Yang X, Liang L, Zhang XF, Jia HL, Qin Y, Zhu XC, et al. MicroRNA-26a suppresses tumor growth and metastasis of human hepatocellular carcinoma by targeting interleukin-6-Stat3 pathway. Hepatology. 2013;58(1):158-70.
64. Zhu Y, Lu Y, Zhang Q, Liu JJ, Li TJ, Yang JR, et al. MicroRNA-26a/b and their host genes cooperate to inhibit the G1/S transition by activating the pRb protein. Nucleic acids research. 2012;40(10):4615-25.
65. Gao J, Li L, Wu M, Liu M, Xie X, Guo J, et al. MiR-26a inhibits proliferation and migration of breast cancer through repression of MCL-1. PloS one. 2013;8(6):e65138.
66. Zhang Y, Wang Z, Gemeinhart RA. Progress in microRNA delivery. Journal of controlled release : official journal of the Controlled Release Society. 2013;172(3):962-74.
67. Chen Y, Gao DY, Huang L. In vivo delivery of miRNAs for cancer therapy: Challenges and strategies. Advanced drug delivery reviews. 2014;81:128-41.
68. Krutzfeldt J, Rajewsky N, Braich R, Rajeev KG, Tuschl T, Manoharan M, et al. Silencing of microRNAs in vivo with 'antagomirs'. Nature. 2005;438(7068):685-9.
69. Elmen J, Lindow M, Schutz S, Lawrence M, Petri A, Obad S, et al. LNA-mediated microRNA silencing in non-human primates. Nature. 2008;452(7189):896-9.
70. Callegari E, Elamin BK, D'Abundo L, Falzoni S, Donvito G, Moshiri F, et al. Anti-tumor activity of a miR-199-dependent oncolytic adenovirus. PloS one. 2013;8(9):e73964.
71. Amendola M, Passerini L, Pucci F, Gentner B, Bacchetta R, Naldini L. Regulated and multiple miRNA and siRNA delivery into primary cells by a lentiviral platform. Molecular therapy : the journal of the American Society of Gene Therapy. 2009;17(6):1039-52.
72. Dorrance AM, Neviani P, Ferenchak GJ, Huang X, Nicolet D, Maharry KS, et al. Targeting leukemia stem cells in vivo with antagomiR-126 nanoparticles in acute myeloid leukemia. Leukemia. 2015;29(11):2143-53.
73. Li Z, Rana TM. Therapeutic targeting of microRNAs: current status and future challenges. Nature reviews Drug discovery. 2014;13(8):622-38.
74. Masotti A, Miller MR, Celluzzi A, Rose L, Micciulla F, Hadoke PW, et al. Regulation of angiogenesis through the efficient delivery of microRNAs into endothelial cells using polyamine-coated carbon nanotubes. Nanomedicine : nanotechnology, biology, and medicine. 2016;12(6):1511-22.
75. Taccioli C, Garofalo M, Chen H, Jiang Y, Tagliazucchi GM, Di Leva G, et al. Repression of Esophageal Neoplasia and Inflammatory Signaling by Anti-miR-31 Delivery In Vivo. Journal of the National Cancer Institute. 2015;107(11).
76. Ghosh R, Singh LC, Shohet JM, Gunaratne PH. A gold nanoparticle platform for the delivery of functional microRNAs into cancer cells. Biomaterials. 2013;34(3):807-16.
77. Jia XQ, Cheng HQ, Qian X, Bian CX, Shi ZM, Zhang JP, et al. Lentivirus-mediated overexpression of microRNA-199a inhibits cell proliferation of human hepatocellular carcinoma. Cell biochemistry and biophysics. 2012;62(1):237-44.
78. Di Martino MT, Campani V, Misso G, Gallo Cantafio ME, Gulla A, Foresta U, et al. In vivo activity of miR-34a mimics delivered by stable nucleic acid lipid particles (SNALPs) against multiple myeloma. PloS one. 2014;9(2):e90005.

79. Scognamiglio I, Di Martino MT, Campani V, Virgilio A, Galeone A, Gulla A, et al. Transferrin-conjugated SNALPs encapsulating 2'-O-methylated miR-34a for the treatment of multiple myeloma. BioMed research international. 2014;2014:217365.
80. van de Donk NW, Moreau P, Plesner T, Palumbo A, Gay F, Laubach JP, et al. Clinical efficacy and management of monoclonal antibodies targeting CD38 and SLAMF7 in multiple myeloma. Blood. 2016;127(6):681-95.
81. Ibrahim S, Keating M, Do KA, O'Brien S, Huh YO, Jilani I, et al. CD38 expression as an important prognostic factor in B-cell chronic lymphocytic leukemia. Blood. 2001;98(1):181-6.
82. Vaisitti T, Audrito V, Serra S, Buonincontri R, Sociali G, Mannino E, et al. The enzymatic activities of CD38 enhance CLL growth and trafficking: implications for therapeutic targeting. Leukemia. 2015;29(2):356-68.
83. Perez-Galan P, Dreyling M, Wiestner A. Mantle cell lymphoma: biology, pathogenesis, and the molecular basis of treatment in the genomic era. Blood. 2011;117(1):26-38.
84. Bende RJ, Smit LA, Bossenbroek JG, Aarts WM, Spaargaren M, de Leval L, et al. Primary follicular lymphoma of the small intestine: alpha4beta7 expression and immunoglobulin configuration suggest an origin from local antigen-experienced B cells. The American journal of pathology. 2003;162(1):105-13.
85. Colomo L, Loong F, Rives S, Pittaluga S, Martinez A, Lopez-Guillermo A, et al. Diffuse large B-cell lymphomas with plasmablastic differentiation represent a heterogeneous group of disease entities. The American journal of surgical pathology. 2004;28(6):736-47.
86. Ansari MQ, Dawson DB, Nador R, Rutherford C, Schneider NR, Latimer MJ, et al. Primary body cavity-based AIDS-related lymphomas. American journal of clinical pathology. 1996;105(2):221-9.
87. Horenstein AL, Durelli I, Malavasi F. Purification of clinical-grade monoclonal antibodies by chromatographic methods. Methods Mol Biol. 2005;308:191-208.
88. Miotto E, Saccenti E, Lupini L, Callegari E, Negrini M, Ferracin M. Quantification of circulating miRNAs by droplet digital PCR: comparison of EvaGreen- and TaqMan-based chemistries. Cancer epidemiology, biomarkers & prevention : a publication of the American Association for Cancer Research, cosponsored by the American Society of Preventive Oncology. 2014;23(12):2638-42.

FIGURES LEGENDS

Figure 1. In the Eμ-*TCL1*FL TG mouse, the leukemic population (B220+/CD5dim) is CD38+. Cells were isolated from the spleen of an adult Eμ-*TCL1*FL transgenic mouse (upper panels) or a transplanted FVB-*TCL1* mouse (lower panels). The left panels show the lymphocyte population, the middle panels the B220+/Cd5dim leukemic population. The right panels show the CD38+ lymphocytes within the B220+/CD5dim population: more than 98% of the cells are positive.

Figure 2. Bio-distribution of miR-181 after the use of CD38-NPs as an *in vivo* delivery agent. (**A**) Bio-distribution 24 hours after intraperitoneal injection of miR-181b mimics (100 μg) delivered into a transplanted FVB-*TCL1* mouse with a high level of disease by the use of CD38-NP, regular nanoparticles (NPs), or Jet-PEI. (**B**) Highlights of splenocytes and liver. Treatment with CD38-NPs induces the most significant increase in the miR-181b level in splenocytes compared with other tissues or methods of delivery (** $p < 0.001$, * $p < 0.05$, respectively), likely reflecting the high number of CD38+ leukemic lymphocytes present in this organ. The results are normalized to SNO412 expression.

Figure 3. Pro-apoptotic activity of different miRNA mimics/AMOs in leukemic splenocytes *in vitro*. (**A**) The apoptotic activity of miRNAs/anti-miRNAs in leukemic splenocytes was evaluated by the Muse Cell Analyzer using the Muse Annexin V & Dead Cell Assay 48 hours after transfection. Statistical assessment of each miRNA effect is referred to the Scramble control. *= $p < 0.05$ (t-test). (**B**) The level of each miRNA after transfection was assessed by ddPCR at the time when apoptosis measured. miRNA levels were normalized on SNO412 and non-transfected cells (UNT).

Figure 4. CD38-NPs mediate an *in vivo* more effective functional outcome than non-conjugated NPs. Forty-eight hours after a single injection of miR-26a mimics (100 ug) with CD38-NPs or non-conjugated NPs, mice with established leukemia were sacrificed, splenocytes were isolated and analyzed for RNA and protein expression. CD38-NP-miRNA26a produced a higher level of miR-26a than NP-miR26a. The results are shown as relative expression of miR-26a normalized to SNO412 expression, as measured by ddPCR. As a result, the treatment with CD38-NPs could mediate more effective functional outcomes as revealed by a clearer apoptotic effect (cleavage of PARP) and a stronger down regulation of a miR-26a target (CDK6).

Figure 5. Apoptotic activity of miRNA/anti-miRNA molecules after a single *in vivo* treatment of mice with established leukemia. Mice with established leukemia were sacrificed 48 hours after a single treatment with miRNA/anti-miRNA molecules. Splenocytes were isolated to evaluate apoptosis. (**A**) Using an Annexin V assay, we observed a significant increase in the percentage of apoptotic cells 48 hours after treatment with CD38-NP-miR-26a ($p = 0.013$), CD38-NP-miR-130a ($p = 0.03$), or CD38-NP-anti-miR-155 ($p = 0.002$). (**B**) At the same time, the relative expression of miR-16, miR-26a, miR-155, miR-130a, miR-34a, and miR-21 was measured in splenocytes by using ddPCR. The results are shown as the relative expression level, normalized to SNO412 expression.

Figure 6. miR-26a exhibits the strongest activity against Eμ-*TCL1*FL leukemic cells. Percentages of circulating leukemic cells were measured just before starting treatments and 48 hours after their completion. The differences between these points were acquired and plotted for each mouse enrolled in the study. miR-26a exhibited the strongest effect on expansion of leukemic burden, as shown in the graph and by the p-values in the associated table. P-values < 0.05 are highlighted by a grey background. N = number of mice, SD = standard deviation.

Figure 7. Modulation of pro-apoptotic proteins and direct targets of miR-26a *in vivo*. Forty-eight hours after the end of long-term treatments, mice were sacrificed and the spleen collected. Proteins were extracted from splenocytes of CD38-NP-miR-26a-treated and control mice for Western blot analysis. (**A**) Cleaved PARP and cleaved caspase-7 are evidence of apoptosis and were clearly visible in the samples treated with miR-26a, but not in the controls. (**B**) The direct molecular activity of miR-26a was demonstrated by showing that two of its known targets, Mcl1 and Cdk6, were down-modulated in the samples treated with miR-26a, but not in the control.

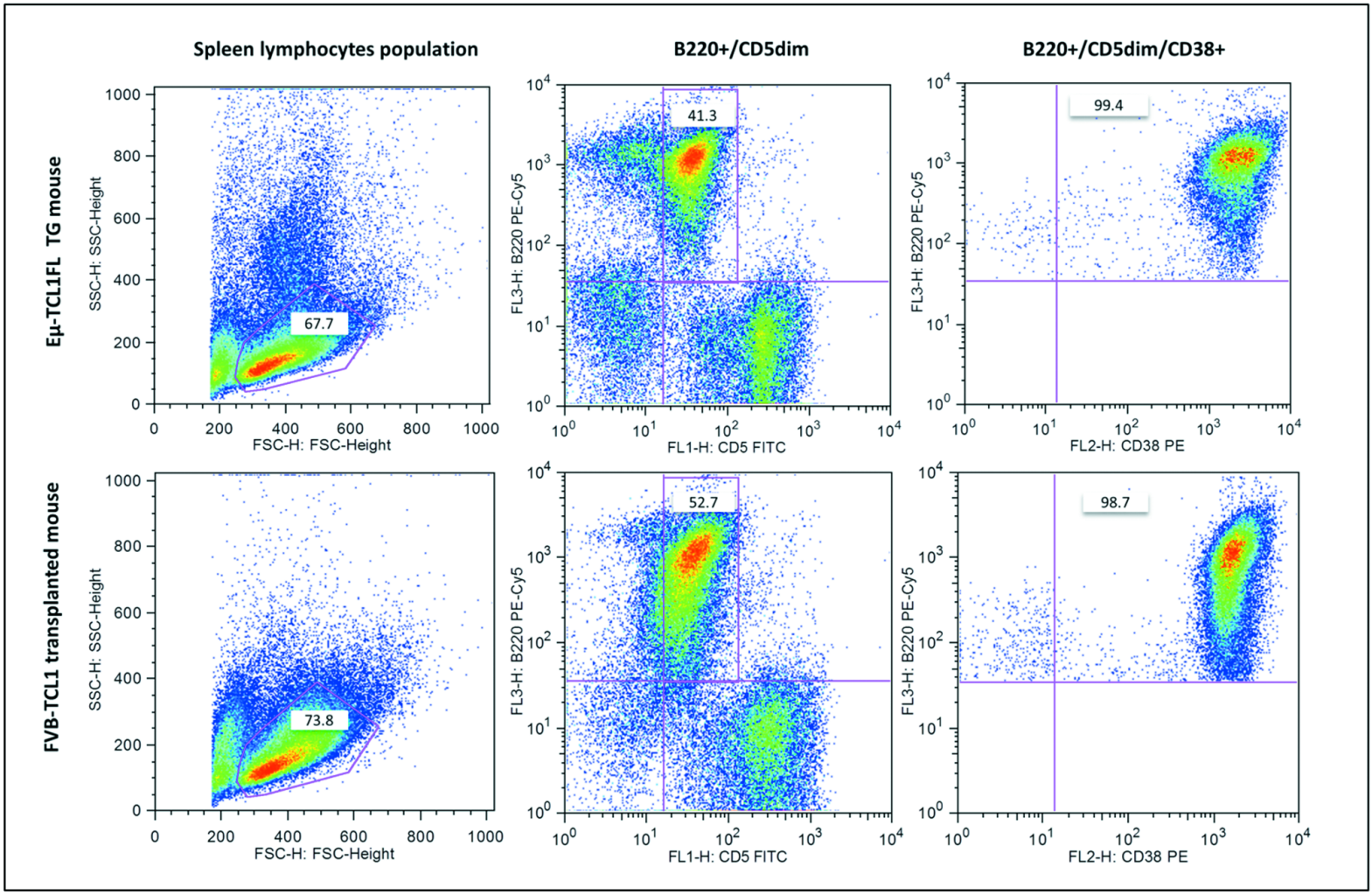
Spleen lymphocytes population
B220+/CD5dim
B220+/CD5dim/CD38+
Eμ-TCL1FL TG mouse
FVB-TCL1 transplanted mouse
SSC-H: SSC-Height
FSC-H: FSC-Height
FL3-H: B220 PE-Cy5
FL1-H: CD5 FITC
FL2-H: CD38 PE
67.7
41.3
99.4
73.8
52.7
98.7

Figure 1

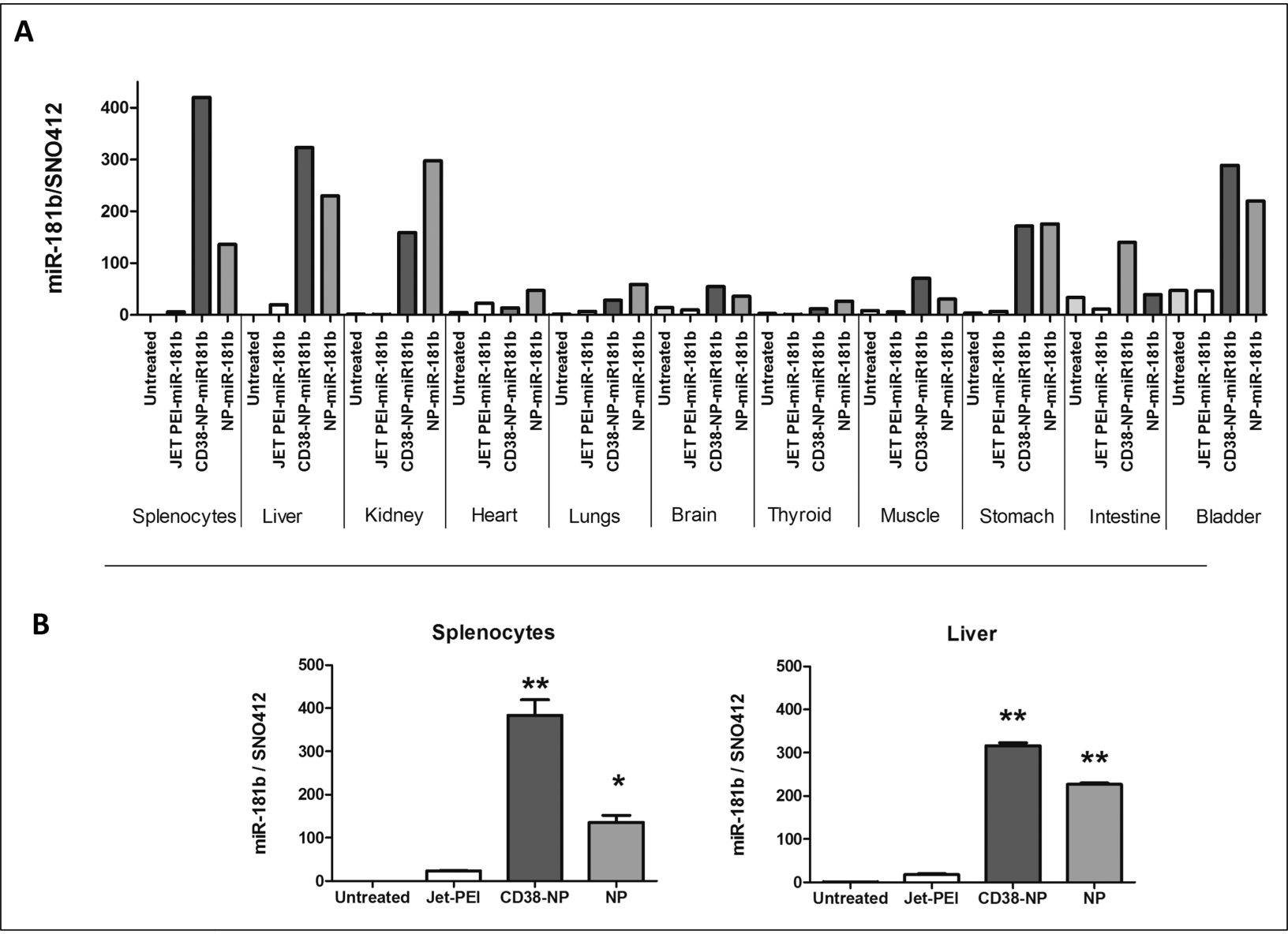
A
miR-181b/SNO412
400
300
200
100
0
Untreated
JET PEI-miR-181b
CD38-NP-miR181b
NP-miR-181b
Splenocytes
Liver
Kidney
Heart
Lungs
Brain
Thyroid
Muscle
Stomach
Intestine
Bladder
B
Splenocytes
miR-181b / SNO412
500
400
300
200
100
0
**
*
Untreated
Jet-PEI
CD38-NP
NP
Liver
miR-181b / SNO412
500
400
300
200
100
0
**
**
Untreated
Jet-PEI
CD38-NP
NP

Figure 2

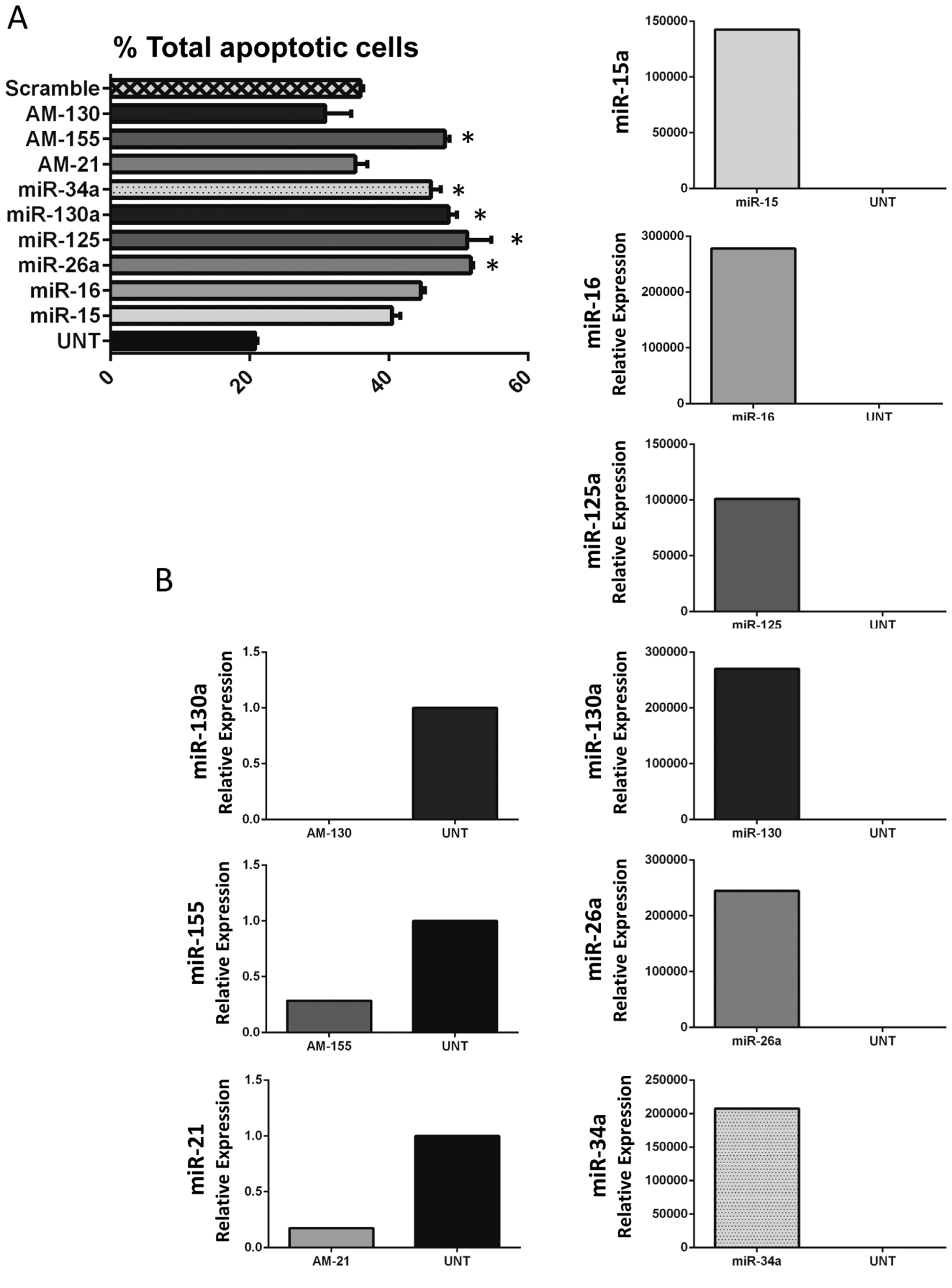
A
% Total apoptotic cells
Scramble
AM-130
AM-155
AM-21
miR-34a
miR-130a
miR-125
miR-26a
miR-16
miR-15
UNT
0
20
40
60
*
*
*
*
*
B
miR-15a
150000
100000
50000
0
miR-15
UNT
miR-16
Relative Expression
300000
200000
100000
0
miR-16
UNT
miR-125a
Relative Expression
150000
100000
50000
0
miR-125
UNT
miR-130a
Relative Expression
1.5
1.0
0.5
0.0
AM-130
UNT
miR-130a
Relative Expression
300000
200000
100000
0
miR-130
UNT
miR-155
Relative Expression
1.5
1.0
0.5
0.0
AM-155
UNT
miR-26a
Relative Expression
300000
200000
100000
0
miR-26a
UNT
miR-21
Relative Expression
1.5
1.0
0.5
0.0
AM-21
UNT
miR-34a
Relative Expression
250000
200000
150000
100000
50000
0
miR-34a
UNT

Figure 3

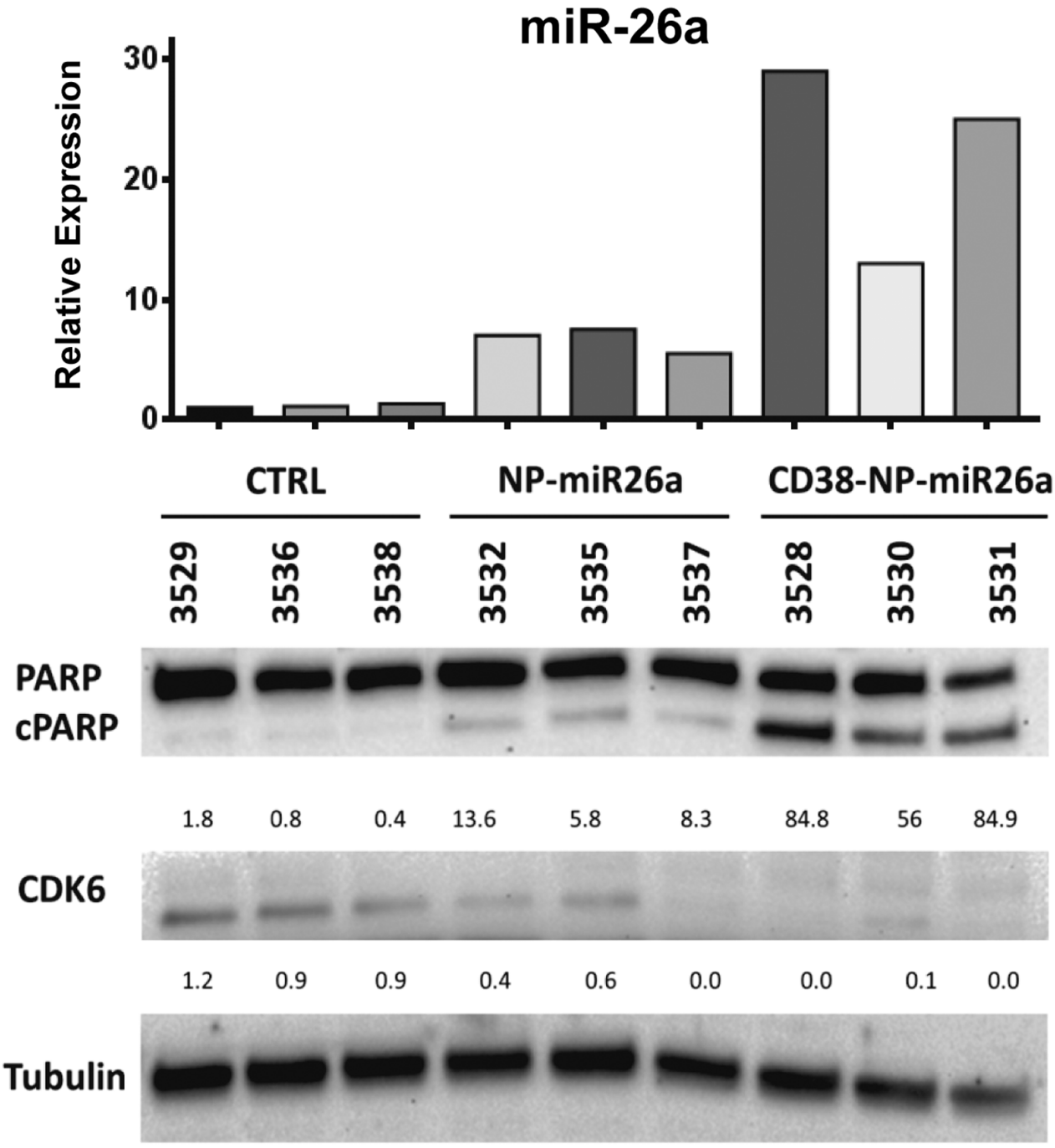
miR-26a
Relative Expression
30
20
10
0
CTRL
NP-miR26a
CD38-NP-miR26a
3529
3536
3538
3532
3535
3537
3528
3530
3531
PARP
cPARP
1.8
0.8
0.4
13.6
5.8
8.3
84.8
56
84.9
CDK6
1.2
0.9
0.9
0.4
0.6
0.0
0.0
0.1
0.0
Tubulin

Figure 4

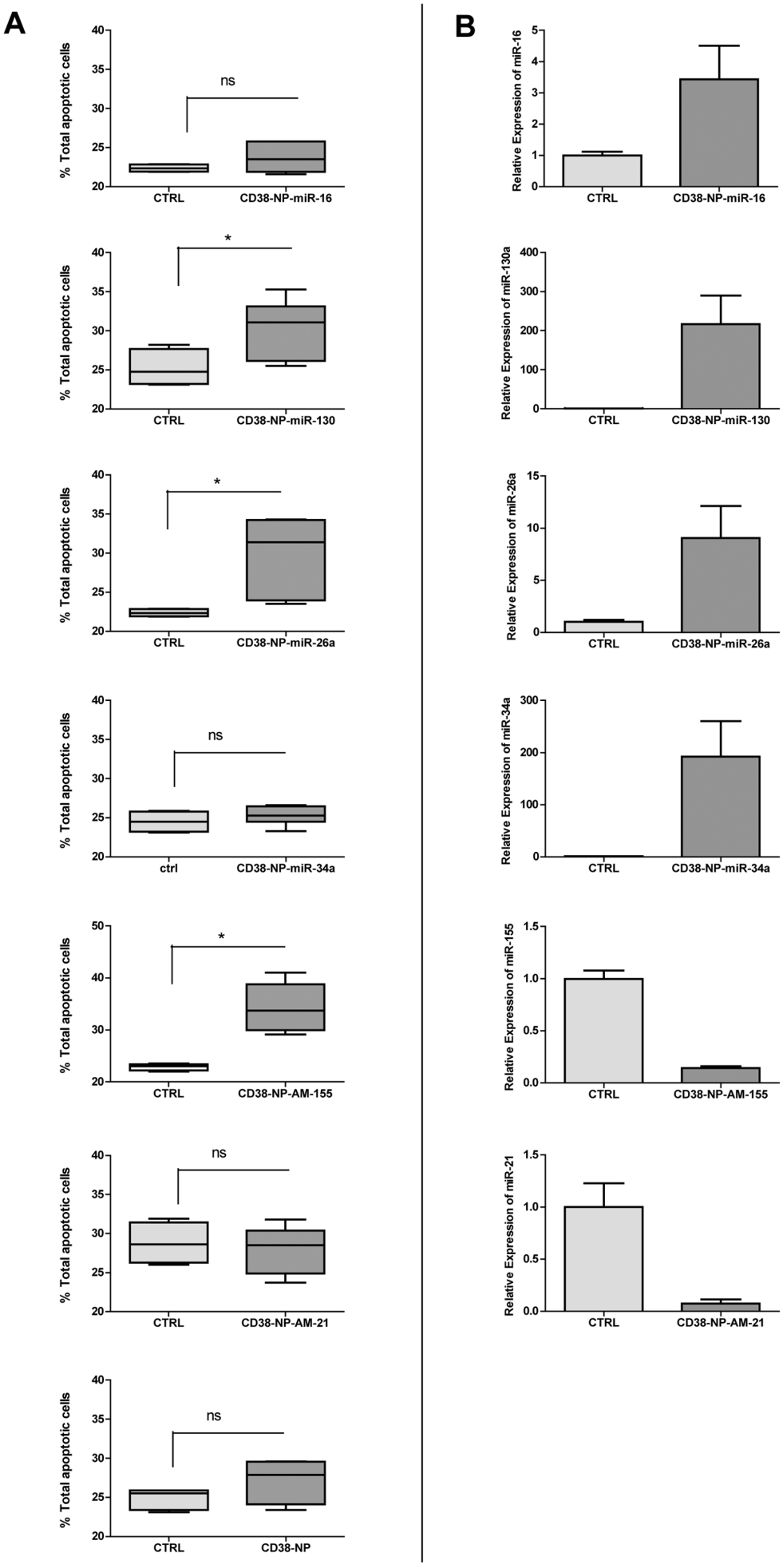
A
% Total apoptotic cells
ns
CTRL
CD38-NP-miR-16
*
CD38-NP-miR-130
CD38-NP-miR-26a
ns
ctrl
CD38-NP-miR-34a
*
CD38-NP-AM-155
ns
CD38-NP-AM-21
ns
CD38-NP
B
Relative Expression of miR-16
CD38-NP-miR-16
Relative Expression of miR-130a
CD38-NP-miR-130
Relative Expression of miR-26a
CD38-NP-miR-26a
Relative Expression of miR-34a
CD38-NP-miR-34a
Relative Expression of miR-155
CD38-NP-AM-155
Relative Expression of miR-21
CD38-NP-AM-21

Figure 5

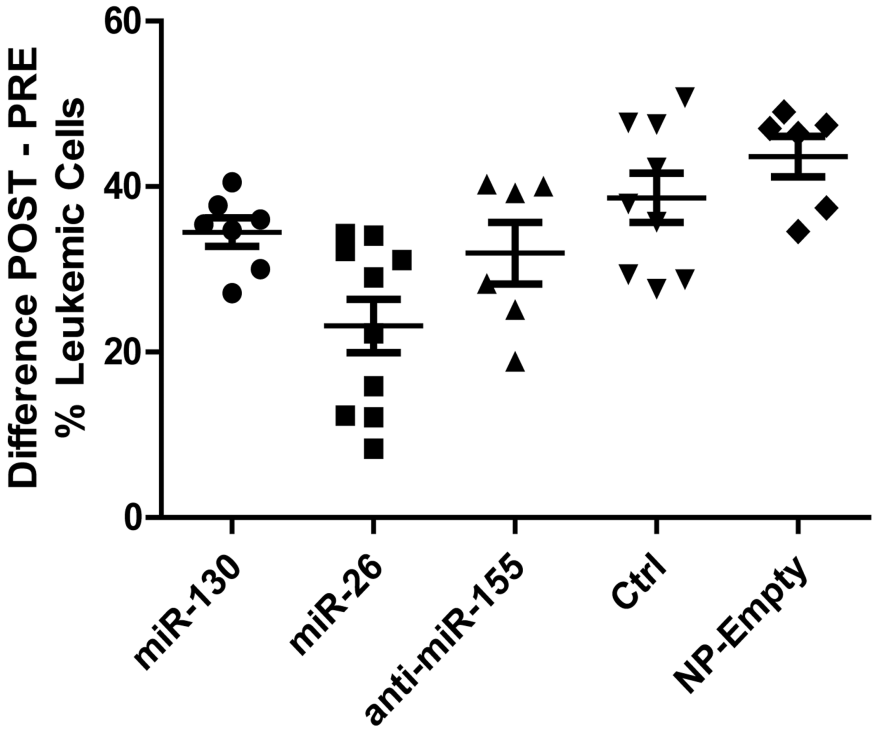

		Leukemia Burden Difference post-pre		t-tests				
	N	Mean	SD	mR-26a	miR-130a	anti-miR-155	Ctrl	CD38-NP-empty
mR-26a	10	23.1	3.2	1.00E+00	**8.30E-03**	1.00E-01	**2.60E-03**	**2.00E-04**
miR-130a	7	34.5	1.7	**8.30E-03**	1.00E+00	5.32E-01	2.49E-01	**1.36E-02**
anti-miR-155	6	32.0	3.7	1.00E-01	5.32E-01	1.00E+00	1.83E-01	**2.61E-02**
Ctrl	9	38.6	3.0	**2.60E-03**	2.49E-01	1.83E-01	1.00E+00	2.53E-01
CD38-NP-empty	6	43.6	2.5	**2.00E-04**	**1.36E-02**	**2.61E-02**	2.53E-01	1.00E+00

Figure 6

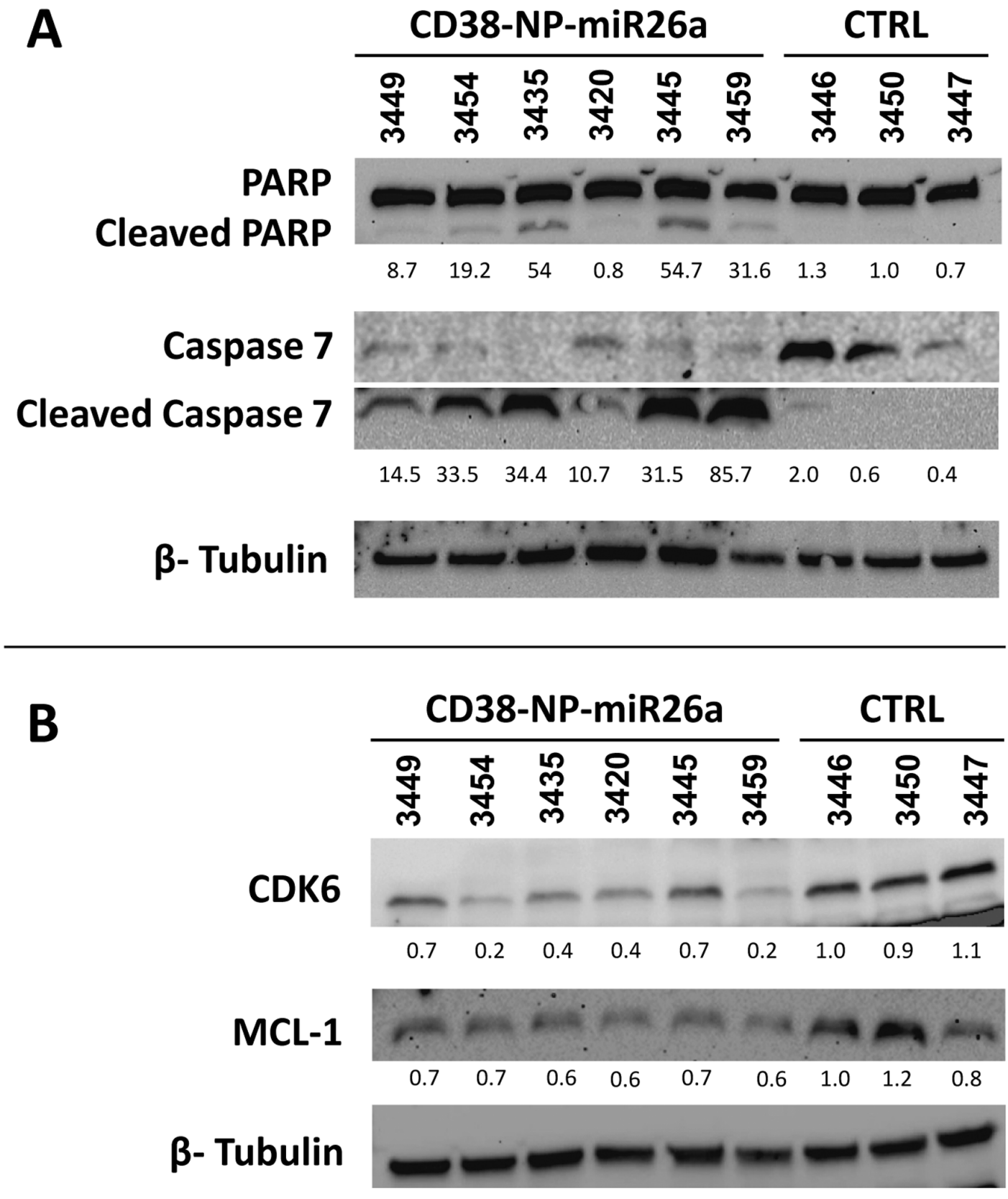
A
CD38-NP-miR26a
CTRL
3449
3454
3435
3420
3445
3459
3446
3450
3447
PARP
Cleaved PARP
8.7
19.2
54
0.8
54.7
31.6
1.3
1.0
0.7
Caspase 7
Cleaved Caspase 7
14.5
33.5
34.4
10.7
31.5
85.7
2.0
0.6
0.4
β- Tubulin
B
CD38-NP-miR26a
CTRL
3449
3454
3435
3420
3445
3459
3446
3450
3447
CDK6
0.7
0.2
0.4
0.4
0.7
0.2
1.0
0.9
1.1
MCL-1
0.7
0.7
0.6
0.6
0.7
0.6
1.0
1.2
0.8
β- Tubulin

Figure 7